

Hydrogen diffusion in partially quasicrystalline $\text{Zr}_{69.5}\text{Cu}_{12}\text{Ni}_{11}\text{Al}_{7.5}$

T. Apih,¹ Varsha Khare,² M. Klanjšek,¹ P. Jeglič,¹ and J. Dolinšek¹

¹*J. Stefan Institute, University of Ljubljana, Jamova 39, SI-1000 Ljubljana, Slovenia*

²*LSG2M (UMR 7584), Centre d'Ingénierie des Matériaux, Ecole des Mines, Parc de Saurupt, F-54042 Nancy Cedex, France*

(Received 5 May 2003; published 15 December 2003)

We report on the direct determination of the hydrogen diffusion constant D in the hydrogen-storage quasicrystalline alloy ZrCuNiAl using the technique of nuclear magnetic resonance diffusion in a static fringe field of a superconducting magnet. The diffusion constant of partially quasicrystalline $\text{Zr}_{69.5}\text{Cu}_{12}\text{Ni}_{11}\text{Al}_{7.5}$ exhibits a significant decrease with increasing hydrogen-to-metal ratio H/M , owing to creation of defects in the lattice during hydrogen loading, whereas the actual alloy structure—the amorphous, icosahedral, or approximant—appears to be less important in the hydrogen diffusivity.

DOI: 10.1103/PhysRevB.68.212202

PACS number(s): 61.44.Br, 66.30.Fq, 76.60.-k

A high number of tetrahedrally coordinated interstitial sites within the crystalline structure and the favorable hydrogen chemistry make the Zr- and Ti-based quasicrystals (QC's) attractive hydrogen-storage materials.¹ The most studied example is the TiZrNi icosahedral alloy,²⁻⁶ which can accommodate hydrogen up to the hydrogen-to-metal ratio $H/M \sim 1.6$, similarly to the best crystalline materials. One of the key factors that characterize good hydrogen-storage materials is the ability to get hydrogen into and out of the metal easily and within a reasonable time. This is related to the mobility of hydrogen atoms within the crystalline lattice, so the knowledge of the hydrogen self-diffusion coefficient in a metal host is of high importance. There exist many methods to determine the hydrogen diffusion constant in metal hydrides,⁷⁻⁹ among which nuclear magnetic resonance (NMR) has probably been applied to more hydrides than any other technique. Various NMR techniques, including spin-lattice relaxation in the laboratory, rotating, and dipolar frames, NMR linewidth, and diffusion in a magnetic field gradient are suitable to characterize diffusion coefficients in the range between 10^{-12} and 10^{-4} cm^2/s . Out of these techniques, only the diffusion in a field gradient gives a direct model-independent value of the diffusion constant D , whereas all other techniques yield indirect information, the correlation time τ_c of the fluctuating local magnetic fields. Assuming that τ_c fluctuations arise predominantly from the translational diffusion of hydrogens (which is in many cases a crude and not well justified assumption), the diffusion coefficient may be estimated from the relation $D = f_T a^2 / 6\tau_c$. Here a is the mean jump distance and f_T is the structure-sensitive “tracer correlation function,” ranging usually between 0.5 and 1. Except for some simple structures, a and f_T are not easily obtained. Regarding the NMR diffusion technique in a magnetic field gradient, the most commonly employed method is that of Stejskal and Tanner,¹⁰ which uses pulsed field gradient (PFG). The technically available PFG values limit the sensitivity of this technique to the range $D \geq 10^{-8}$ cm^2/s . The PFG method was successfully applied to simple-structure metal hydrides, such as the elemental⁹ fcc PdH_x and TiH_x and the $\text{Pd}_{1-x}\text{Ag}_x\text{H}_y$ alloys,¹¹ where D was determined at temperatures where its value was in the range 10^{-6} – 10^{-8} cm^2/s . The more complicated structure and/or structural and chemical disorders make the hydrogen diffu-

sion in QC's slower with $D < 10^{-8}$ cm^2/s , so that no direct determination of D in QC's by the PFG method was reported—to the best of our knowledge—in the literature so far. In this paper we present a direct determination of the hydrogen self-diffusion coefficient in the hydrogen-storage ZrCuNiAl QC alloy by using the method of NMR diffusion in a static fringe field (SFF) of a superconducting magnet. Here we apply the SFF method to the study of hydrogen diffusion in QC's.

The SFF method, introduced in the 1990's by Kimmich *et al.*,¹² takes advantage of the ultrahigh magnetic field gradients (typically up to 80 T/m) of the highly stable static fringe field of an NMR superconducting magnet, extending sensitivity to molecular diffusion down to $D \geq 10^{-11}$ cm^2/s . SFF diffusion measurements were successfully applied to systems such as supercooled liquids, molecular crystals, long-chain polymers, and systems of confined mesoscopic geometries and fractal structures,¹³ whereas no reports exist on the measurement of hydrogen diffusion in metal hydrides by this technique. For hydrogen storage QC's, the SFF method offers a promising way to directly determine the hydrogen diffusion coefficient. There, the D values are below the detection threshold of the PFG method at practically all temperatures of interest, because at elevated temperatures (e.g., at 350 °C for² TiZrNi) the icosahedral (i) QC structure decomposes and transforms into more stable crystalline hydride phases.

Our hydrogen diffusion measurements by the SFF method were performed in a quaternary icosahedral alloy $\text{Zr}_{69.5}\text{Cu}_{12}\text{Ni}_{11}\text{Al}_{7.5}$ (in the following abbreviated as $\text{ZrCuNiAl}_{7.5}$). This alloy exhibits exceptional glass forming ability, and is one of the few known systems¹⁴ that undergo transformation from the glassy to the quasicrystalline state by annealing the amorphous as-cast material (melt-spun ribbons) above the glass transition temperature 372 °C. The details of the material preparation, hydrogen loading and desorption, stability, structural quality, and structure transformation upon hydrogenation are published elsewhere.¹⁴⁻¹⁸ During annealing, a microstructure of icosahedral QC's develops within the sea of amorphous material, the largest attainable quasicrystalline volume being $V_{\text{QC}} \approx 90\%$. Since the storage capacity was found higher and the hydrogen absorption kinetics faster for samples with a qua-

sicrystalline volume of about 50% than for the fully quasicrystalline ones¹⁸ (90%), our experiments were conducted on $V_{\text{QC}} \approx 50\%$ samples. The hydrogen diffusion results presented in the following should thus not be considered as specific to the QC phase, but to quasicrystalline microcrystals embedded in an amorphous matrix. The samples were hydrogen loaded electrochemically in a 2:1 glycerine-phosphoric acid at 25 °C and a current density of $j = 10 \text{ A/m}^2$. The hydrogen content was determined by a microbalance with accuracy of $\pm 1 \mu\text{g}$ and from the shift of the x-ray lines¹⁵ towards smaller angles due to lattice expansion. The increase of the quasilattice constant by about 10% at $H/M = 2.0$ in $\text{ZrCuNiAl}_{7.5}$ compares well to the 7% increase observed² in the Ti-based QC's with $H/M = 1.6$. Our study included five samples loaded to different H/M 's: (i) an amorphous as-cast material loaded to $H/M = 0.192$ (hereafter referred to as sample A0.19), where the amorphous material can be loaded to a maximum $H/M = 0.9$ before failure of the ribbon,¹⁶ and four quasicrystalline samples loaded to (ii) $H/M = 0.309$ (QC0.31 sample), (iii) $H/M = 0.50$ (QC0.50), (iv) $H/M = 1.9$ (QC1.9), and (v) $H/M = 2.1$ (QC2.1). Since the amount of hydrogen outgassing soon after the hydrogenation has not been studied, the high H/M values of 1.9 and 2.1 should not be taken literally. An increasing degree of hydrogenation leads to an increased nearest-neighbor distance of both the QC phase and the amorphous matrix, accompanied by a phase transformation of the QC from icosahedral to approximant phases¹⁸ and its final amorphization at H/M values above 1.0. X-ray diffraction and transmission electron microscopy (TEM) investigations¹⁵ showed that, after hydrogen degassing, the quasilattice parameter is restored totally to its initial ($H/M = 0$) value, whereas the remaining weakened contrast of the bright-field TEM images and the absence of weak diffraction lines indicate the presence of a high density of defects, not present in the virgin material. These defects—of still unknown type—are created during hydrogen loading and are not annealed-out after complete hydrogen desorption.

The SFF experiment was conducted in a superconducting magnet with the center field 6.3 T (corresponding to the ^1H resonance frequency of 270 MHz). The experimental setup, including the fringe field data of this magnet, were published recently.¹⁹ The probe head was fine positioned at one edge of the superconducting coil, where the proton resonance frequency amounted $\nu(^1\text{H}) = 100.0 \text{ MHz}$ and the gradient was $g = 49 \text{ T/m}$. The stimulated spin-echo pulse sequence ($\pi/2 - \tau - \pi/2 - t - \pi/2 - \tau - \text{echo}$) was used with the $\pi/2$ rf pulse length of $1 \mu\text{s}$. In the presence of diffusing nuclei in a constant field gradient g , the amplitude of the spin echo decays with time according to¹²

$$A = A_0 \exp(-2\tau/T_2) \exp(-t/T_1) \times \exp\left[-\gamma^2 g^2 D \tau^2 \left(t + \frac{2}{3}\tau\right)\right]. \quad (1)$$

Here A_0 is the initial echo amplitude, T_1 and T_2 are the spin-lattice and spin-spin relaxation times, respectively, γ is the gyromagnetic ratio, and D is the diffusion constant. In

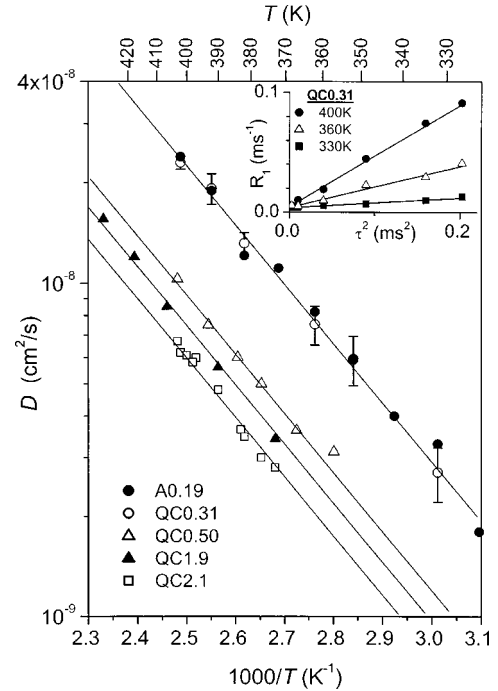


FIG. 1. Temperature-dependent hydrogen diffusion constant D in the $\text{ZrCuNiAl}_{7.5}$ alloy hydrogenated to different H/M (samples described in the text). Solid lines are fits with $D = D_0 \exp(-E_a/k_B T)$, using in all cases the same value of the activation energy $E_a = 365 \text{ meV}$. Typical R_1 vs τ^2 curves, from which D is extracted, are shown as an inset.

order to extract D , one first varies systematically the “diffusion time” t , keeping the time τ fixed. The echo amplitude then decays in t with the constant $R_1 = 1/T_1 + \gamma^2 g^2 D \tau^2$. The experiment is repeated for a set of τ values and the resulting R_1 is plotted as a function of τ^2 . Typical R_1 vs τ^2 curves at different temperatures are shown as an inset in the Fig. 1. The slope of the straight line yields the diffusion constant D , whereas the zero intercept is $1/T_1$, which is independently known from the relaxation-time measurements.

The diffusion constants were determined in the interval between room temperature and 440 K and the data are displayed in Fig. 1. Within this temperature interval, the D values of all samples are in the range between 2×10^{-8} and $1.8 \times 10^{-9} \text{ cm}^2/\text{s}$. The $D(T)$ data points fall on straight lines in the $\ln D$ vs $1/T$ plot, indicating a simple classical over-barrier-hopping hydrogen diffusion with $D = D_0 \exp(-E_a/k_B T)$, where E_a is the activation energy. Within our experimental precision ($\sim 10\%$), the $D(T)$ curves of all samples run in parallel, demonstrating that the variation of the activation energy between the samples is smaller than the experimental error. This, however, does not exclude the possible small variation of the E_a with H/M , it is just too small to be detected by the SFF technique. The $D(T)$ fits (solid lines in Fig. 1) are all made with the same value of the activation energy $E_a = 365 \pm 15 \text{ meV}$ (which should be considered as the average E_a of all samples). Here it is important to stress that this E_a value is model independent and hence does not suffer from the model-dependent analysis as in the case when extracted from the τ_c data of the NMR relaxation

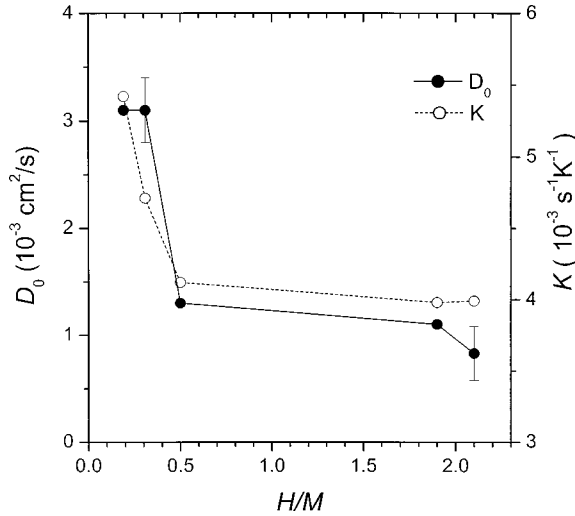


FIG. 2. The H/M dependence of the diffusion prefactor D_0 (solid circles) and the Korringa constant K (open circles).

experiments. The translational shifts of the $D(T)$ curves show that the prefactors $D_0 \approx a^2/6\tau_\infty$ [where τ_∞^{-1} is the hydrogen jump attempt frequency defined by the Arrhenius relation $\tau_c = \tau_\infty \exp(E_a/k_B T)$] are different. Samples loaded to higher H/M values show systematically lower D_0 values (Fig. 2). This result demonstrates that the main difference in the hydrogen diffusivity within the samples hydrogenated to different H/M 's and also showing structural differences (the starting material is amorphous whereas the QC samples undergo an icosahedral-to-approximant-to-amorphous transformation¹⁸ upon hydrogenation with increasing H/M) comes predominantly from the prefactor D_0 and not from the difference in the activation energies. This is not a trivial result, as one would expect that the increased nearest-neighbor separation due to lattice expansion with increased H/M would increase the potential barriers between adjacent hydrogen interstitial sites, so that E_a should increase at higher H/M . In contrast, the results of Fig. 1 suggest that the decreased diffusivity for increasing H/M originates predominantly from the decrease of D_0 , whereas the change in the activation energy—if present—plays only a minor role. The diffusivity is also fairly independent of the actual crystalline structure (D values of the starting amorphous material A0.19 and the quasicrystalline QC0.31 sample, both loaded to small H/M , are practically equal), whereas it is strongly dependent on the amount of hydrogen loaded, being smaller for larger H/M 's. A trivial explanation could be the “site-blocking” effect, where the increased occupancy of the interstitial sites for increasing $H/M = x$ would result in a decrease of the attempt jump frequency as⁹ $(2-x)\tau_\infty^{-1}$ (where 2 is taken as the maximum possible x for the $\text{ZrCuNiAl}_{7.5}$), so that the diffusion coefficient scales with x as $D = (2-x)D_0 \exp(-E_a/k_B T)$. This should lead to a linear decrease of the prefactor $(2-x)D_0$ with increasing H/M , in contrast to a much faster variation of the experimental D_0 values displayed in Fig. 2. According to this, the H/M dependence of D_0 may not be explained by the simple site-blocking effect. The decrease of D_0 with H/M can also not

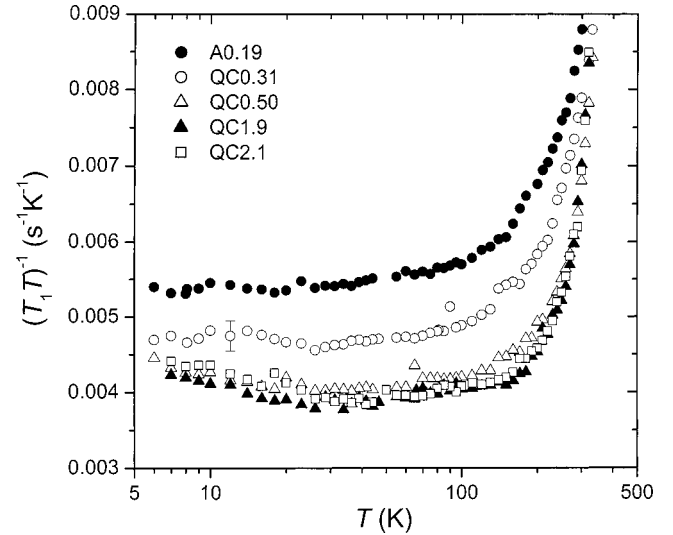


FIG. 3. The ^1H spin-lattice relaxation rates of the investigated $\text{ZrCuNiAl}_{7.5}$ samples in the temperature interval from 420 to 4 K in a $(T_1 T)^{-1}$ vs T plot. The constant plateaus below 100 K demonstrate the dominance of the conduction-electron relaxation contribution at low temperatures, whereas the $(T_1 T)^{-1}$ increase above 100 K is due to the dipole-dipole contribution.

be attributed to the gradual amorphization of the QC samples upon the hydrogenation-induced phase transformation to the amorphous state, as the amorphous sample A0.19 shows in fact the highest diffusivity, equal to that of the QC0.31 sample. This unconventional hydrogen diffusivity decrease for increasing H/M can be consistently explained by considering the above discussed TEM—and x-ray detected defects in the lattice, introduced by the hydrogen loading, to be at the origin of this phenomenon. The defects locally distort the tetrahedral coordination of the interstitial sites, making the number of available hydrogen sites smaller with increasing H/M . The concentration of defects strongly depends on H/M , but is rather independent of the actual crystalline structure (as tetrahedral sites are present in all phases—the QC, the approximant, and the amorphous). This hypothesis is supported indirectly by the low-temperature measurements of the NMR nuclear spin-lattice relaxation rate T_1^{-1} . In metal hydrides, the ^1H relaxation rate usually contains two terms,⁹ $T_1^{-1} = T_{1c}^{-1} + T_{1d}^{-1}$, where T_{1d}^{-1} is the nuclear dipole-dipole contribution and T_{1c}^{-1} is the conduction-electron relaxation rate that becomes by far dominant at low temperatures. The conduction-electron rate obeys the well-known relation $(T_{1c} T)^{-1} = K$ with K being the Korringa constant that is related to the density of electronic states (DOS) at the Fermi level $K \propto g^2(E_F)$. The relaxation rates of all samples are displayed in Fig. 3 in a $(T_1 T)^{-1}$ vs T plot. The horizontal $(T_1 T)^{-1} = \text{const}$ lines below 100 K demonstrate the dominance of the conduction-electron relaxation rate at low temperatures. The height of the plateau of each sample is determined by the value of its respective Korringa constant. In Fig. 2, the K values are displayed, as a function of H/M , on the same plot together with the D_0 . The constants K exhibit a decreasing behavior for increasing H/M in a very much the same manner as the diffusion prefactor D_0 . This K behavior

can be again qualitatively explained by the defects-induced distortion of the lattice, which decreases the electronic DOS function $g(E_F)$ and hence the Korringa constant. The creation of defects in the lattice upon hydrogenization thus consistently explains the temperature dependence of both the diffusion prefactor D_0 and the Korringa constant K . The fact that D_0 and K show strong dependence on H/M , but do not depend significantly on the actual structure of the samples demonstrates that the influence of quasiperiodicity on the

hydrogen diffusion in the $\text{ZrAlCuNi}_{7.5}$ alloy is of minor importance. The main reason for decreased hydrogen diffusivity in samples loaded to higher H/M values appears to be the lattice distortion (that is not just a simple uniform expansion) due to defect creation upon hydrogenation.

We thank Professor U. Köster from Dortmund for provision of the samples and for reading the manuscript prior to submission.

-
- ¹See, for a review, P. C. Gibbons and K. F. Kelton, in *Physical Properties of Quasicrystals*, edited by Z. M. Stadnik, Vol. 126 of *Springer Series in Solid-State Sciences* (Springer, Berlin, 1999), p. 403.
- ²A. M. Viano, R. M. Stroud, P. C. Gibbons, A. F. McDowell, M. S. Conradi, and K. F. Kelton, *Phys. Rev. B* **51**, 12 026 (1995).
- ³A. Shastri, E. H. Majzoub, F. Borsa, P. C. Gibbons, and K. F. Kelton, *Phys. Rev. B* **57**, 5148 (1998).
- ⁴K. R. Faust, D. W. Pfitsch, N. A. Stojanovich, A. F. McDowell, N. L. Adolphi, E. H. Majzoub, J. Y. Kim, P. C. Gibbons, and K. F. Kelton, *Phys. Rev. B* **62**, 11 444 (2000).
- ⁵K. Foster, R. G. Leisure, J. B. Shaklee, J. Y. Kim, and K. F. Kelton, *Phys. Rev. B* **61**, 241 (2000).
- ⁶A. F. McDowell, N. L. Adolphi, and C. A. Sholl, *J. Phys.: Condens. Matter* **13**, 9799 (2001).
- ⁷J. Völkl and G. Alefeld, in *Diffusion in Solids, Recent Developments*, edited by A. S. Nowick and J. J. Burton (Academic, New York, 1975), p. 231.
- ⁸J. Völkl and G. Alefeld, in *Hydrogen in Metals I-Basic Properties*, edited by G. Alefeld and J. Völkl (Springer, Berlin, 1978), p. 321.
- ⁹R. C. Bowman, Jr., in *Metal Hydrides*, edited by G. Bambakidis, NATO ASI Series B, Vol. 76 (Plenum, New York, 1981), p. 109.
- ¹⁰E. O. Stejskal and J. E. Tanner, *J. Chem. Phys.* **42**, 288 (1965).
- ¹¹H. Züchner, H. Barlag, and G. Majer, *J. Alloys Compd.* **330–332**, 448 (2002).
- ¹²R. Kimmich, W. Unrath, G. Schnur, and E. Rommel, *J. Magn. Res.* **91**, 136 (1991).
- ¹³I. Chang, F. Fujara, B. Geil, G. Hinze, H. Sillescu, and A. Toelle, *J. Non-Cryst. Solids* **172–174**, 674 (1994).
- ¹⁴U. Köster, J. Meinhardt, S. Roos, and H. Liebertz, *Appl. Phys. Lett.* **69**, 179 (1996).
- ¹⁵B. I. Wehner, J. Meinhardt, U. Köster, H. Alves, N. Eliaz, and D. Eliezer, *Mater. Sci. Eng.* **A226–228**, 1008 (1997).
- ¹⁶D. Zander, H. Leptien, U. Köster, N. Eliaz, and D. Eliezer, *J. Non-Cryst. Solids* **250–252**, 893 (1999).
- ¹⁷D. Zander, U. Köster, N. Eliaz, D. Eliezer, and D. Plachke, in *Quasicrystals*, MRS Symposia Proceedings No. 553, edited by J. M. Dubois, P. A. Thiel, A. P. Tsai, and K. Urban (Materials Research Society, Warrendale, 1999), p. 49.
- ¹⁸D. Zander, U. Köster, and V. Khare, MRS Symposia Proceedings No. 643, edited by E. Belin-Ferré, P. A. Thiel, A. P. Tsai, and K. Urban (Materials Research Society, Warrendale, 2001), p. K2.2.1.
- ¹⁹P. Jeglič, A. Lebar, T. Apih, and J. Dolinšek, *J. Mater. Res.* **150**, 39 (2001).